Relationship Between Retention Index in Dual-Phase ^{18}F-FDG PET, and Hexokinase-II and Glucose Transporter-1 Expression in Pancreatic Cancer

Tatsuya Higashi, MD, PhD[1]; Tsuneo Saga, MD, PhD[1]; Yuji Nakamoto, MD, PhD[1]; Takayoshi Ishimori, MD[1]; Marcelo H. Mamede, MD[1]; Michihiko Wada, MD, PhD[2]; Ryuichiro Doi, MD, PhD[2]; Ryo Hosotani, MD, PhD[2]; Masayuki Imamura, MD, PhD[2]; and Junji Konishi, MD, PhD[1]

[1]Department of Nuclear Medicine and Diagnostic Imaging, Graduate School of Medicine, Kyoto University, Kyoto, Japan; and [2]Department of Surgery and Surgical Basic Science, Graduate School of Medicine, Kyoto University, Kyoto, Japan

Recently, some studies have shown that delayed scanning with ^{18}F-FDG PET may help to differentiate malignant from benign pancreatic lesions. However, no study has evaluated the relationship between temporal changes in ^{18}F-FDG uptake and expression of hexokinase or glucose transporter. **Methods:** Twenty-one consecutive patients with pancreatic cancer were studied preoperatively by dual-phase ^{18}F-FDG PET, performed 1 and 2 h after injection of ^{18}F-FDG. The standardized uptake value (SUV) of the pancreatic cancer was determined, and the retention index (RI) (%) was calculated by subtracting the SUV at 1 h (SUV1) from the SUV at 2 h (SUV2) and dividing by SUV1. The percentages of cells strongly expressing hexokinase type-II (HK-II) and glucose transporter-1 (GLUT-1) were scored on a 5-point scale (1 = 0%–20%, 2 = 20%–40%, 3 = 40%–60%, 4 = 60%–80%, 5 = 80%–100%) by visual analysis of immunohistochemical staining of paraffin sections from the tumor specimens using anti-HK-II and anti-GLUT-1 antibody (HK-index and G-index, respectively). **Results:** SUV2 (mean ± SD, 5.7 ± 2.6) was higher than SUV1 (5.1 ± 2.1), with an RI of 8.5 ± 11.0. Four cases of cancer, in which SUV2 showed a decline from SUV1, showed a low HK-index (1.8 ± 1.1), whereas 4 cases with an RI of ≥20 and 13 cases with an intermediate RI (0–20) showed significantly higher HK-indices (4.3 ± 0.7 and 3.1 ± 1.5, respectively; $P < 0.05$). RI showed a positive correlation with HK-index, with an R^2 of 0.27 ($P < 0.05$), but no significant correlation with the G-index. SUV1 showed no relationship with the HK-index but showed a weak positive correlation with the G-index, with an R^2 of 0.05 ($P = 0.055$). **Conclusion:** These preliminary findings suggest that the RI obtained from dual-phase ^{18}F-FDG PET can predict HK-II expression and that the SUV (at 1 h) has a positive correlation with GLUT-1 expression but not with HK-II expression.

Imaging with ^{18}F-FDG PET has been used as a powerful evaluation modality in oncologic nuclear medicine (*1–6*), not only for detecting tumors but also for monitoring therapy (*7,8*), for staging (*9–10*), and for grading (*11*). Emission scans are usually obtained ≤1 h after ^{18}F-FDG administration in oncologic ^{18}F-FDG PET. Recently, several studies showed that delayed scanning (≥90 min after ^{18}F-FDG administration) with ^{18}F-FDG PET may help to differentiate between malignant and benign lesions (*12–15*). In these studies, ^{18}F-FDG accumulation constantly increased up to 3–4 h in many cases, whereas in a few cases it fell 1 h after ^{18}F-FDG administration. These temporal changes in ^{18}F-FDG uptake in the tumor may arise from the balance of expression of glucose transporters and glycolytic enzymes in tumor cells. However, no study has evaluated the expression of these transporters and enzymes in relation to the ^{18}F-FDG uptake kinetics. Hexokinase-II (HK-II) and glucose transporter-1 (GLUT-1) are known as major subtypes of each family for many cancer cells (*16–19*). This retrospective study investigated the usefulness of dual-phase ^{18}F-FDG PET scanning (1 and 2 h) as a noninvasive preoperative tool to evaluate HK-II and GLUT-1 expression in pancreatic cancer.

MATERIALS AND METHODS

Patients

The study group comprised 21 consecutive patients with pancreatic cancer (13 men, 8 women; age range, 40–82 y; mean age, 60.8 ± 8.9 y) of 27 patients with malignant disease reported previously (*15*). Surgical resection or needle biopsy during laparotomy confirmed the histologic diagnosis. (Five patients without

an appropriate surgical specimen for immunohistochemical evaluation were excluded from this study.) The diseases included 17 cases of invasive ductal adenocarcinoma, 3 cases of pancreatic mucinous cystadenocarcinoma, and 1 case of intraductal papillary carcinoma. Before being enrolled in this study, each patient gave written informed consent, as required by the Kyoto University Human Study Committee.

PET Study

[18]F was produced by a [20]Ne (d, α) ^{18}F nuclear reaction, and ^{18}F-FDG was synthesized by the acetyl hyprofluorite method (20). PET was performed using a whole-body PET camera (PCT3600W; Hitachi Medico, Tokyo, Japan) that had 8 rings, which provided 15 tomographic sections at 7-mm intervals. The intrinsic resolution was 4.6 mm in full width at half maximum at the center, and the axial resolution was 7 mm at half maximum. The effective resolution after reconstruction was approximately 10 mm. The patients fasted for at least 5 h before the ^{18}F-FDG injection. The exact position of the pancreatic lesion was confirmed and marked on the skin using sonography before PET examination. The patients were placed supine on the center of the PET table. During the entire imaging procedure, they kept their arms over their head in the same position, aided by a headrest and a holding bar. This patient position was determined and marked with 8 corresponding points in a cross line with a pen using a laser beam alignment system, as the center of the tumor was located in the center of the imaging field. The patient was then fixed in place with a holding belt across the abdomen. Each patient underwent transmission scanning for attenuation correction for 11 min. After the transmission scan was obtained, approximately 370 MBq (10 mCi) ^{18}F-FDG were administered intravenously, and serial static scanning was performed for 12 min at 2 time points, 1 h (54–72 min) and 2 h later (114–135 min). At the time of emission scanning, the subject was repositioned on the PET table. The marking and the laser beam system were used to ensure that the patient was placed in precisely the same position as in the transmission scan. Serum levels of glucose were monitored immediately before the ^{18}F-FDG injection. Initially, PET images were compared with the corresponding CT images, which permitted accurate identification of the tumor relative to anatomic landmarks, for example, the upper and lower part of the kidney, the shape of the liver, and the gallbladder bed. ^{18}F-FDG accumulation was analyzed semiquantitatively by calculating the standardized uptake value (SUV) in the regions of interest placed over the suspected lesions on 1- and 2-h images (SUV [at 1 h] and SUV [at 2 h]) after injection of ^{18}F-FDG (15).

The region of interest placed over the tumor was 10×10 mm (independent of tumor size) and was placed in tumor areas that showed the highest ^{18}F-FDG activity. We defined the retention index (RI) (%) as follows: RI = $100 \times$ (SUV [at 2 h] − SUV [at 1 h])/SUV (at 1 h).

Histologic Examination

All patients underwent surgical resection or needle biopsy during laparotomy. Three or more paraffin sections per patient were processed for anti-GLUT-1 or anti-HK-II immunostaining or routine hematoxylin staining. The polyclonal rabbit anti–glucose transporter antibody reactive with human GLUT-1 (brain/erythrocyte type) was purchased from DAKO (Carpinteria, CA). It was raised against 12-amino-acid synthetic peptide corresponding to the carboxyl terminus of human GLUT-1 (21). It undergoes immunoreaction with a 50-kDa glucose transporter species in human

erythrocytes and in a variety of human cancer cells. It was diluted 1:200 with 0.05 mol/L Tris-HCl buffer containing a carrier protein and 0.015 mol/L sodium azide (DAKO). The polyclonal rabbit antihexokinase antibody reactive with rat HK-type II isozyme (HK-II) was purchased from Chemicon International, Inc. (Temecula, CA). It was raised against synthetic peptide corresponding to the carboxyl terminus of rat HK-II (22). It undergoes immunoreaction with a 10-kDa hexokinase species in a variety of human cancer cells. It was diluted 1:500 with 0.05 mol/L Tris-HCl buffer containing a carrier protein and 0.015 mol/L sodium azide.

Paraffin was removed from sections of each tumor using xylene and ethanol. Before immunohistochemical procedures, unmasking treatments were performed on all sections. Sections for anti-GLUT-1 immunostaining were incubated with Target Retrieval Solution (DAKO), using the water bath method at 95°C–99°C for 20 min. The other sections, including those for anti-HK-II immunostaining, were unmasked by the microwave method (strong range) using a distilled water bath for 15 min (5 min for each of 3 times).

After 20 min for cooling, the sections were washed with phosphate-buffered saline (PBS) (DAKO), containing 20 mmol/L sodium phosphate and 150 mmol/L NaCl (pH 7.0), for 15 min (5 min for each of 3 times). Then, the endogenous peroxidase activities were blocked for 10 min at 25°C with 0.3% hydrogen peroxide in distilled water and were washed with the PBS for 5 min. The nonspecific binding was blocked for 30 min at 25°C with blocking buffer (DAKO), which contained 10% normal bovine serum in PBS. In the next step, each section was incubated with the anti-GLUT-1 antibody or anti-HK-II antibody as a primary antibody for 1 h at 25°C. Parallel sections were incubated with healthy rabbit IgG (20 μg/mL) as negative controls. Then, all the sections were washed with PBS with 0.05% polyoxyethylene sorbitan monolaurate (Tween 20; Kanto Chemical Co., Tokyo, Japan) for 15 min (5 min for each of 3 times). In the following steps, each section was stained by the horseradish peroxidase (HRP)-labeled polymer method, using an Envision Kit/HRP 3,3′-diaminobenzidine tetrahydrochloride (DAB) (DAKO). For linking, the sections were incubated with the labeled polymer for 60 min at 25°C and washed with PBS with 0.05% Tween 20 for 15 min (5 min for each of 3 times). As a substrate-chromogen solution, DAB was used at 25°C for 10 min, diluted at 1 mg/mL with 0.05 mol/L Tris-HCl buffer, pH 7.5. All sections were then rinsed gently with distilled water and washed in flowing water for 5 min. In the final step, the sections were lightly counterstained with Gill's hematoxylin and then dehydrated, the alcohol was removed, and a coverslip was positioned with mounting medium. Other chemicals not mentioned were of the highest purity available. All slides were examined by light microscopy.

Data Analysis

Immunohistochemical analysis for anti-GLUT-1 antibody and anti-HK-II antibody was independently performed 3 times by a well-experienced physician who was unaware of the SUVs. In each analysis, the percentages of strongly immunoreactive tumor cells in the total tumor cells were visually analyzed for each of 10 low-power fields (magnification, 10×10) or more (up to 30 fields), and the averaged percentage was calculated and scored on a 5-point scale (1 = 0%–20%, 2 = 20%–40%, 3 = 40%–60%, 4 = 60%–80%, 5 = 80%–100%) for each counting trial. Then, the 3 scores from all 3 counting trials were averaged again to give the

TABLE 1
Patient Characteristics

Patient no.	Sex	Age (y)	Histologic diagnosis	Differentiation	Operation	SUV (at 1 h)	SUV (at 2 h)	RI
1	F	71	Invasive ductal carcinoma	Well	Resectable	2.82	2.48	−12.06
2	M	68	Invasive ductal carcinoma	Poorly	Unresectable*	3.16	2.84	−10.13
3	F	58	Invasive ductal carcinoma	Poorly	Unresectable*	3.58	3.35	−6.42
4	M	52	Invasive ductal carcinoma	Moderately	Resectable	3.06	2.90	−5.23
5	F	66	Invasive ductal carcinoma	Moderately	Resectable	4.99	5.14	3.01
6	M	58	Invasive ductal carcinoma	Poorly	Unresectable*	5.24	5.43	3.63
7	M	70	Invasive ductal carcinoma	Poorly	Resectable	4.78	5.06	5.86
8	M	62	Invasive ductal carcinoma	Moderately	Resectable	4.42	4.72	6.79
9	M	62	Invasive ductal carcinoma	Moderately/poorly	Unresectable*	3.76	4.04	7.45
10	M	49	Invasive ductal carcinoma	Poorly	Unresectable*	3.73	4.02	7.77
11	M	57	Invasive ductal carcinoma	Poorly	Unresectable*	5.85	6.44	10.09
12	F	82	Invasive ductal carcinoma	Moderately	Unresectable*	4.26	4.70	10.33
13	M	53	Invasive ductal carcinoma	Poorly	Resectable	9.34	10.51	12.53
14	F	68	Invasive ductal carcinoma	Moderately/poorly	Unresectable*	10.76	12.67	17.75
15	M	58	Invasive ductal carcinoma	Moderately	Resectable	4.86	5.96	22.63
16	F	62	Invasive ductal carcinoma	Moderately	Unresectable*	7.68	9.47	23.31
17	M	54	Invasive ductal carcinoma	Well	Unresectable*	6.00	7.75	29.17
18	M	59	Mucinous cystadenocarcinoma	Well	Resectable	4.24	4.63	9.20
19	F	64	Mucinous cystadenocarcinoma	Well	Unresectable*	6.54	7.34	12.23
20	F	40	Mucinous cystadenocarcinoma	Well	Resectable	3.41	4.19	22.87
21	M	63	Intraductal papillary carcinoma	Well	Resectable	4.83	5.16	6.83

*Needle biopsy under laparotomy.

GLUT-1 expression index (G-index) or HK-II expression index (HK-index).

One section from each tumor, processed with a nonspecific IgG as a negative control, was visually analyzed twice for tumor cellularity by a well-experienced physician who was unaware of the SUVs. In each analysis, tumor cellularity was scored on a 5-point scale (1 = low, 2 = low to moderate, 3 = moderate, 4 = moderate to high, 5 = high) by visual analysis for each of 10 low-power fields or more (up to 30 fields), and the averaged score was then calculated and scored on a 5-point scale. Two of each score from each counting trial were averaged again to give the tumor cell cellularity index (C-index). The data were statistically analyzed by nonparametric analysis using the Mann-Whitney test and the Spearman rank correlation.

RESULTS

Clinical and PET Findings

No patients had hyperglycemia. Table 1 summarizes the clinical and PET findings and the routine histologic diagnoses for the 21 patients. Ten patients underwent tumor resection. The others underwent a partial resection or open biopsy for advanced pancreatic cancer, with gastrojejunostomy or other anastomoses, or intraoperative radiation therapy, or both. The SUV increased 2 h after injection in 17 of 21 lesions but decreased in 4 lesions. The SUV at 2 h (mean ± SD, 5.7 ± 2.6) tended to be higher than the SUV at 1 h (5.1 ± 2.1), with an RI of 8.5 ± 11.0. There was no significant relationship between histologic diagnosis, differentiation, stage of disease, operative procedure, and each of the ^{18}F-FDG PET quantitative findings. Figure 1 shows the

relationship between SUV (at 1 h) and the RI obtained from dual-phase ^{18}F-FDG PET. They correlated positively: Tumors with higher SUVs had higher RIs ($P < 0.05$). No patient had an RI of ≥30%, and no patient with a negative RI had an SUV (at 1 h) of ≥4.0.

Immunohistochemical Findings

Table 2 summarizes the findings of the immunohistochemical analysis using anti-GLUT-1 and anti-HK-II anti-
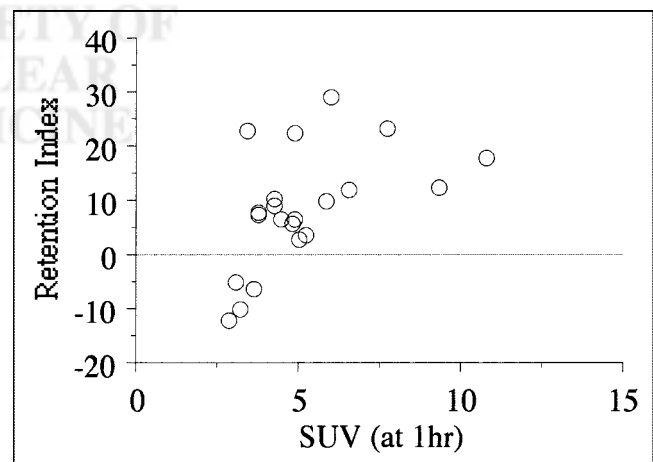
FIGURE 1. Results of SUV at 1 h and RI of dual-phase ^{18}F-FDG PET. Positive correlation existed between SUV at 1 h and RI ($P < 0.05$). Four patients with negative RI showed low SUVs at 1 h.

TABLE 2
TABLE 2
Results of Immunohistochemistry and Tumor Cellularity

| Patient no. | GLUT-1 (G-index) | | | | HK-II (HK-index) | | | | Cellularity (C-index) | | |
| | Average | Counting trial | | | Average | Counting trial | | | Average | Counting trial | |
		First	Second	Third		First	Second	Third		First	Second
1	1.0	1	1	1	1.0	1	1	1	3.0	3	3
2	1.0	1	1	1	1.3	1	2	1	1.5	1	2
3	3.0	3	3	3	1.3	2	1	1	5.0	5	5
4	1.0	1	1	1	3.3	3	3	4	2.5	3	2
5	1.3	1	2	1	1.0	1	1	1	2.5	2	3
6	2.7	2	3	3	4.7	4	5	5	5.0	5	5
7	4.0	4	4	4	3.3	3	4	3	1.5	1	2
8	5.0	5	5	5	4.0	3	4	5	2.5	3	2
9	1.0	1	1	1	1.3	2	1	1	2.0	2	2
10	3.3	4	3	3	5.0	5	5	5	5.0	5	5
11	3.7	4	3	4	3.0	4	2	3	5.0	5	5
12	1.0	1	1	1	2.7	4	2	2	3.0	3	3
13	5.0	5	5	5	5.0	5	5	5	4.5	5	4
14	2.0	3	2	1	2.0	2	2	2	5.0	5	5
15	4.3	4	4	5	4.0	3	4	5	3.0	3	3
16	1.3	1	2	1	3.3	3	4	3	4.0	4	4
17	3.7	3	4	4	5.0	5	5	5	2.5	3	2
18	1.0	1	1	1	1.7	3	1	1	4.0	5	3
19	1.3	1	2	1	2.0	2	2	2	2.0	2	2
20	2.7	2	3	3	4.7	4	5	5	4.0	4	4
21	4.0	4	4	4	5.0	5	5	5	2.0	2	2

body (G-index and HK-index, respectively) and the findings of the histologic analysis of C-index. In the G-index, 3 counting trials showed similar scores in 10 patients. In another 10 patients, the scores varied within 1 point. Only in 1 patient (patient 14) did the scores vary from 3 to 1. In the HK-index, 3 counting trials showed the same score in 8 patients. In another 8 patients, the scores varied within 1 point. In the other 5 patients, the scores varied within 2 points. No patient had a 3-point variance between counting trials. These findings showed that intraobserver variance was negligible. The C-index also showed no significant intraobserver variance.

When patients were categorized according to the result of RI (negative RI, RI of 0–20, RI > 20), the HK-index in four patients with a negative RI (1.8 ± 1.1) were lower than those of 4 patients with an RI of ≥ 20 (4.3 ± 0.7) and also lower than those of 13 patients with an intermediate RI (0–20) (3.1 ± 1.5). The HK-index differed significantly between these 3 groups ($P < 0.05$). No significant difference was seen between the G-index of patients with a negative RI (1.5 ± 1.0), patients with an intermediate RI (0–20) (2.7 ± 1.5), and patients with an RI ≥ 20 (3.0 ± 1.3). Figure 2 shows the comparative analysis of immunohistochemical staining results using anti-GLUT-1 and anti-HK-II antibody (G-index and HK-index). The G-index and the HK-index had a close positive correlation ($P < 0.005$).

Figure 3 shows the comparative analysis between immunohistochemical findings (G-index and HK-index) and the parameters of dual-phase ^{18}F-FDG PET (SUV at 1 h and RI). A weak positive relationship existed between the G-

index and the SUV at 1 h ($P = 0.055$), whereas no significant correlation existed between HK-index and SUV (at 1 h). However, the RI did not show a significant correlation with the G-index but did show a close relationship with the HK-index ($P < 0.05$). No significant correlation was found between the C-index and any other index. Figures 4 and 5 show 2 examples of ^{18}F-FDG PET images and immunohistochemical staining of GLUT-1 glucose transporter and HK-II hexokinase for pancreatic cancer cases with a lower RI and a higher RI.

R^2 = 0.491
p=0.0022
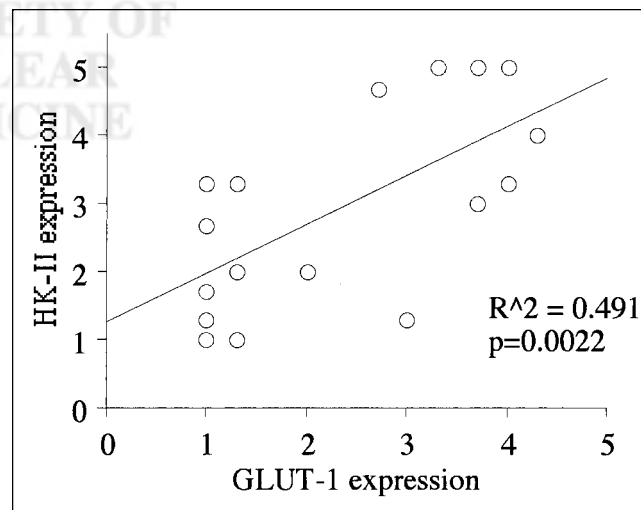
FIGURE 2. Results of immunohistochemical staining using anti-GLUT-1 and anti-HK-II. They correlated closely ($P < 0.005$).
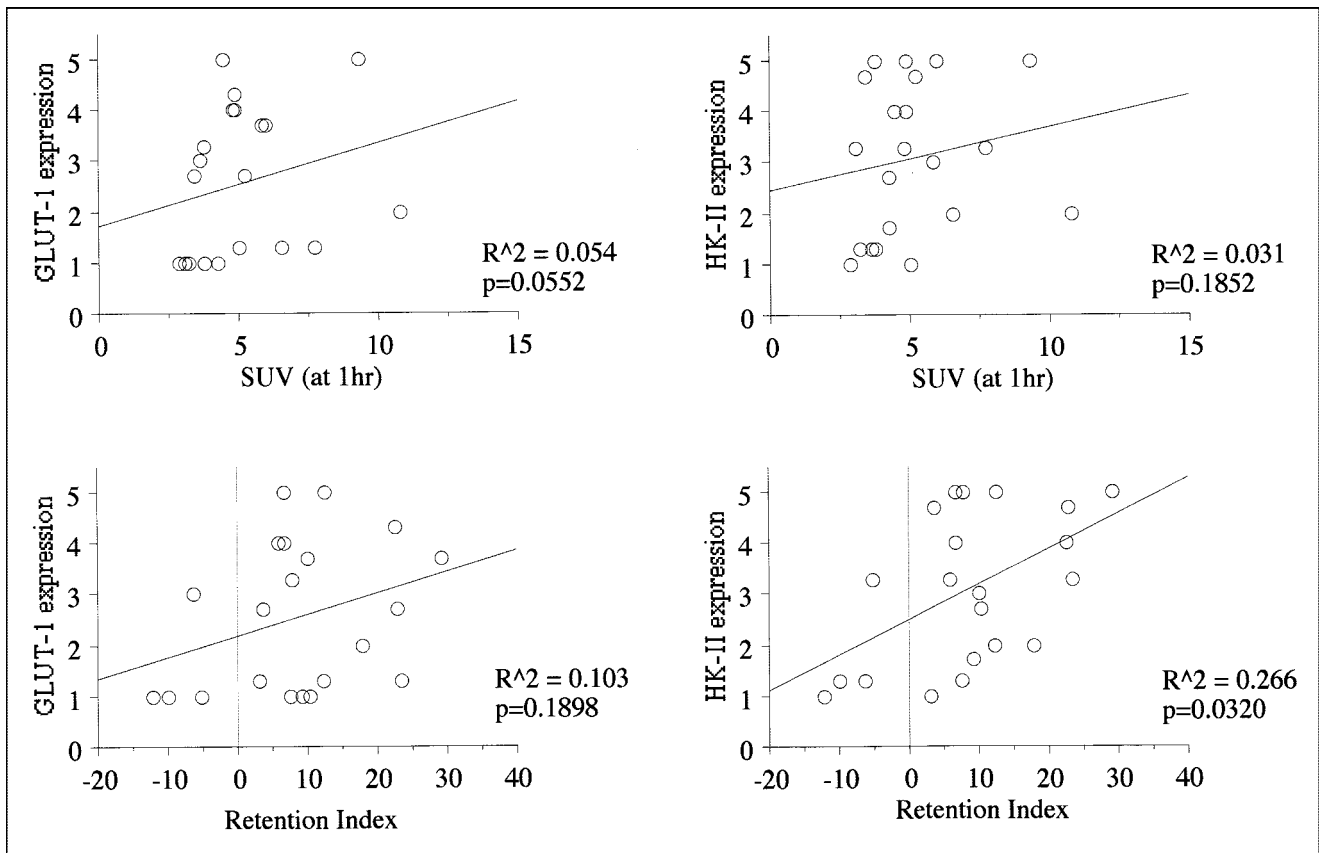
FIGURE 3. Results of comparative analysis between quantitative values of dual-phase ^{18}F-FDG PET and immunohistochemical staining. SUV at 1 h showed a weak positive correlation with GLUT-1 glucose transporter expression ($P = 0.055$), whereas no significant relationship was found between SUV at 1 h and HK-II hexokinase expression. However, RI had no significant relationship with GLUT-1 glucose transporter expression, whereas RI and HK-II hexokinase expression had significant positive relationship ($P < 0.05$).

DISCUSSION

Although ^{18}F-FDG PET has been accepted as a powerful noninvasive diagnostic modality for evaluating various tumors, the usefulness of dual-phase or late-phase ^{18}F-FDG PET has not been established (*12–15*). ^{18}F-FDG is generally administered intravenously under fasting conditions, and the tumor imaging is performed ≤1 h after the intravenous injection. A variety of studies using dynamic ^{18}F-FDG PET have been reported and showed that detailed analysis of the 3-compartment model could provide several prognostic values in the management of cancer patients (*3,23,24*). More typically, semiquantitative image analysis using the SUV has been applied for evaluation of PET findings, because this parameter can be determined relatively easily by a single, short static emission scan, without an hour-long dynamic acquisition or arterial blood sampling (*25*). Cancer imaging using static scans with determination of the SUV is easy to perform, helpful for cancer patients, and of essential clinical value in oncology and has played an important role in the dissemination of ^{18}F-FDG PET technology. However, many studies have indicated limitations of the SUV as a clinical tool in oncology, such as false-positive findings in cases of inflammatory lesions (*26–28*). The SUV overlap

between malignant and benign lesions is significant, and a single SUV figure at a certain time point cannot elucidate the dynamics of ^{18}F-FDG accumulation in a lesion. Although some studies have reevaluated the usefulness of dynamic ^{18}F-FDG PET in oncology—to clarify whether the procedure increases diagnostic accuracy or adds some clinical value compared with a static scan and SUV—the procedure is complex and time consuming and is not suitable for clinical oncology (*29,30*). For obtaining more information within a reasonable scanning time, this kind of dual-phase ^{18}F-FDG PET is a realistic method from a practical, clinical standpoint. In the protocol of this study, an additional 12 min of scanner time were necessary for the dual-phase PET scan of only 1 patient (only a 5- to 10-min extension was needed in our recent protocol using a whole-body PET scanner with a different acquisition method). Thus, dual-phase ^{18}F-FDG PET is worth considering to evaluate the dynamics of ^{18}F-FDG accumulation in a lesion and to obtain possible prognostic values for the management of cancer patients.

In this retrospective study, we evaluated 2 factors that were suggested to be responsible for the ^{18}F-FDG accumulation mechanism in tumor tissue: the expression of HK-II
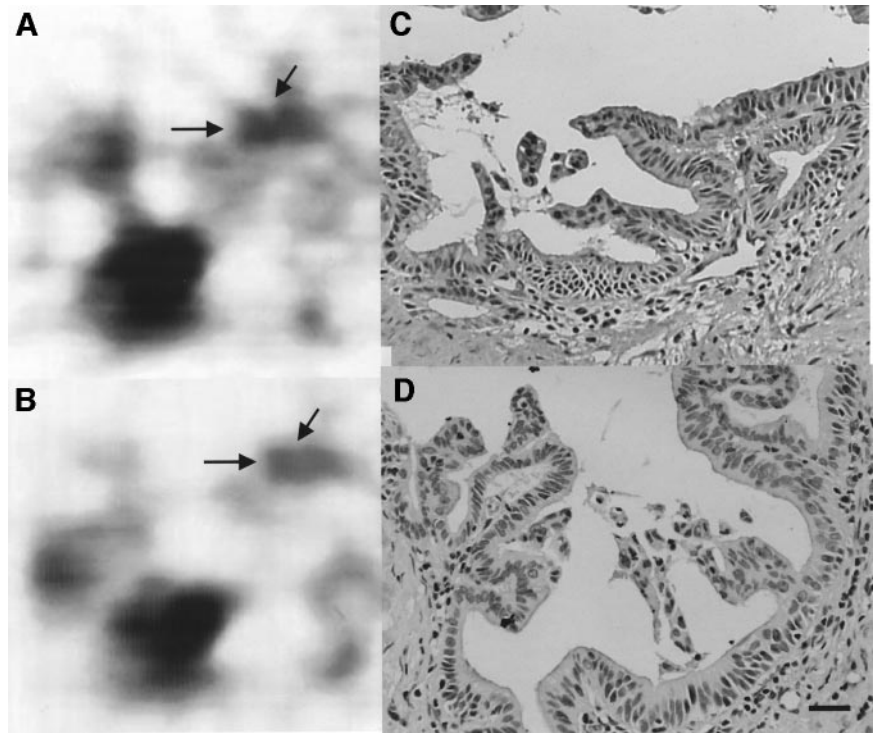
FIGURE 4. Invasive ductal adenocarcinoma (arrows) in pancreatic head of patient 1. ^{18}F-FDG PET images obtained at 1 h, when tumor SUV was 2.82 (A), and at 2 h, when tumor SUV was 2.48 (B), with RI of −12.1%. Immunohistochemical staining of GLUT-1 (C) and of HK-II (D) shows no significant strong expression of GLUT-1 or HK-II. Percentages of strong expressed cells of both proteins were scored as <20%. (×400; bar = 20 μm)

and the expression of GLUT-1. Among the family of hexokinases and glucose transporters, HK-II and GLUT-1 were selected because each is known as a major subtype of each family for various cancer cells and for various cancer tissues (16–19). A close correlation exists between GLUT-1 and HK-II expression (Fig. 2). Tumor cells or transformed cells

are known to have enhanced anaerobic glycolysis as a whole, which requires both glucose transporter overexpression and enhanced hexokinase activity, although the relative importance (as the rate-limiting step) of these 2 factors is still controversial (31–34). The present findings indicated that expression of both GLUT-1 and HK-II increased as the
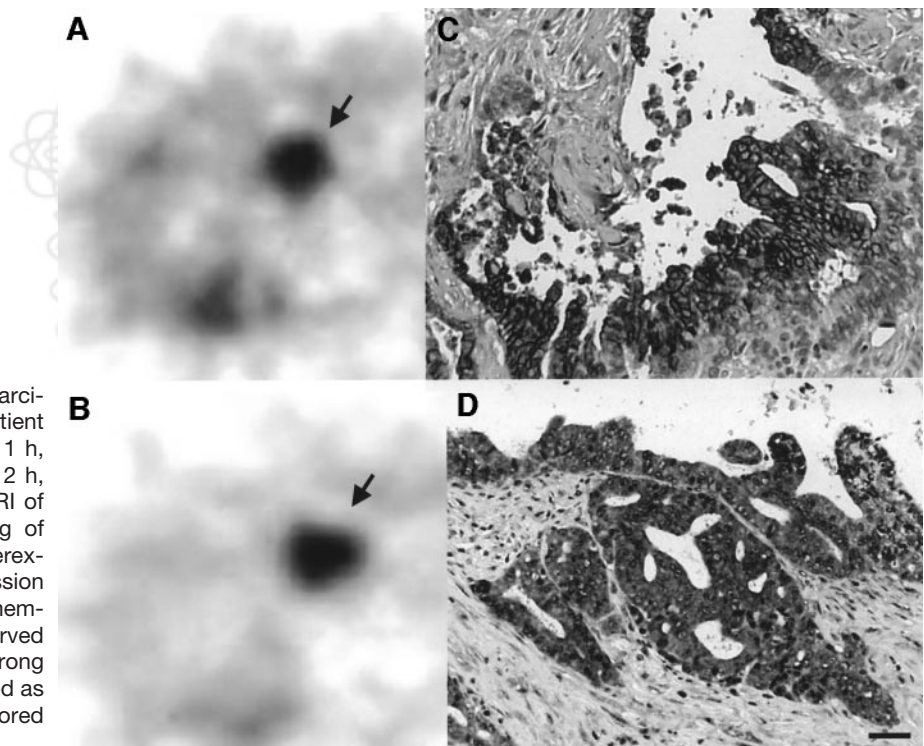
FIGURE 5. Invasive ductal adenocarcinoma (arrows) in pancreatic head of patient 17. ^{18}F-FDG PET images obtained at 1 h, when tumor SUV was 6.0 (A), and at 2 h, when tumor SUV was 7.75 (B), with RI of 29.2%. Immunohistochemical staining of GLUT-1 (C) and of HK-II (D) shows overexpression of GLUT-1 and HK-II. Expression of GLUT-1 is observed mainly in membrane, whereas that of HK-II is observed mainly in cytoplasm. Percentages of strong expressed cells of GLUT-1 were scored as 50%–80%, and those of HK-II were scored as >80%. (×400; bar = 20 μm)

enhanced anaerobic glycolysis rose, whereas there appeared to be an imbalance between them in some cases (Table 2). The findings also suggested that the RI calculated by dual-phase ^{18}F-FDG PET could predict HK-II expression and might be an indicator of the phosphorylation rate. In the late phase after ^{18}F-FDG injection, only a low concentration of ^{18}F-FDG remains in the blood or in the interstitial space. Glucose transporters are facilitative diffusion carriers locating across the plasma membrane that accelerate the transport of glucose down its concentration gradient by facilitative diffusion, a form of passive transport, between cytosol of tumor cells and blood or the interstitial space (35). If ^{18}F-FDG uptake of tumor cells is still increasing during the late phase, the concentration of ^{18}F-FDG in the cytosol of tumor cells should be much lower than that in the blood system or interstitial space, and free ^{18}F-FDG in the cytosol should be phosphorylated to ^{18}F-FDG-6-phosphate rapidly inside the tumor cells by hexokinase. Therefore, the concept that overexpression of hexokinase is associated with a high RI has considerable validity. On the other hand, four patients with negative retention indices all had low SUV values. Two of these patients had low GLUT-1 and low HK-II, whereas a third had high GLUT-1 and low HK-II and a fourth had low GLUT-1 and high HK-II. Further study would be needed for evaluation of the glycolytic mechanism in cases of low ^{18}F-FDG uptake, including background activity of surrounding tissues. In this study, a close correlation was also found between the SUV at 1 h and GLUT-1 expression. These findings are compatible with our previous findings for pancreatic tumors despite the difference in histologic analyzing methods (19,36). However, the SUV at 1 h did not correlate with HK-II expression. Therefore, SUV at 1 h may be considered an indicator of GLUT-1 expression grade but not an indicator of HK-II. Thus, the present findings suggest that dual-phase ^{18}F-FDG PET can predict 2 important factors in cellular glycolysis of cancers: GLUT-1 glucose transporter expression and HK-II hexokinase expression. Furthermore, our results have important implications for the evaluation of repeated ^{18}F-FDG PET studies during follow-up after treatment. For example, if the first study were performed 1 h after injection of ^{18}F-FDG and the follow-up scan were acquired at 2 h, the comparison between pre- and posttherapeutic PET would be unreliable and misleading.

In this retrospective study, we could not analyze HK-II expression or RI as a prognostic factor because the follow-up period after initial treatment was inadequate. However, some studies have suggested the usefulness of HK activity or the fractional rate constant k3 in the 3-compartment model as a prognostic factor in a variety of cancers (3,37–38). Further follow-up observations are needed in these types of cancer patients.

In the previous study, there were 4 patients with false-positive benign lesions in the differential diagnosis using dual-phase ^{18}F-FDG PET (15). These included 1 patient with acute pancreatitis in whom endoscopic retrograde cholangiopancreatography was performed 3 d before the PET study, 1 patient with acute cholangitis in whom a nasogastric biliary drainage tube had been inserted in the common bile duct, and 2 patients with autoimmune pancreatitis. Evaluation of the histopathologic background of the increasing ^{18}F-FDG uptake during the late phase should be required for these 3 types of inflammatory lesion.

CONCLUSION

We propose the use of a dual-phase ^{18}F-FDG PET static scan in evaluating HK-II and GLUT-1 expression. An additional acquisition at 2 h after injection is beneficial for differentiating between malignant and benign lesions in the pancreas. Also, the additional acquisition obviates a dynamic ^{18}F-FDG PET scan with arterial lines.

REFERENCES

1. Strauss LG, Clorius JH, Schlag P, et al. Recurrence of colorectal tumors: PET evaluation. *Radiology.* 1989;170:329–332.
2. Strauss LG, Conti PS. The applications of PET in clinical oncology. *J Nucl Med.* 1991;32:623–648.
3. Wahl RL, Cody RL, Hutchins GD. Primary and metastatic breast carcinoma: initial clinical evaluation with PET with the radiolabeled glucose analog 2-[^{18}F]-fluoro-2-deoxy-D-glucose. *Radiology.* 1991;179:765–770.
4. Hawkins RA, Hoh C, Dahlbom M, et al. PET cancer evaluations with FDG. *J Nucl Med.* 1991;32:1555–1558.
5. Hoh CK, Hawkins RA, Glaspy JA, et al. Cancer detection with whole-body PET using 2-[^{18}F]fluoro-2-deoxy-D-glucose. *J Comput Assist Tomogr.* 1993;17:582–589.
6. Inokuma T, Tamaki N, Torizuka T, et al. Evaluation of pancreatic tumors with positron emission tomography and F-18 fluorodeoxyglucose: comparison with CT and US. *Radiology.* 1995;195:345–352.
7. Vitola JV, Delbeke D, Meranze SG, Mazer MJ, Pinson CW. Positron emission tomography with F-18-fluorodeoxyglucose to evaluate the results of hepatic chemoembolization. *Cancer.* 1996;78:2216–2222.
8. Findlay M, Young H, Cunningham D, et al. Noninvasive monitoring of tumor metabolism using fluorodeoxyglucose and positron emission tomography in colorectal cancer liver metastases: correlation with tumor response to fluorouracil. *J Clin Oncol.* 1996;14:700–708.
9. Vansteenkiste JF, Stroobants SG, De Leyn PR, et al. Lymph node staging in non-small-cell lung cancer with FDG PET scan: a prospective study on 690 lymph node stations from 68 patients. *J Clin Oncol.* 1998;16:2142–2149.
10. Kole AC, Plukker JT, Nieweg OE, Vaalburg W. Positron emission tomography for staging of oesophageal and gastroesophageal malignancy. *Br J Cancer.* 1998;78:521–527.
11. Adler LP, Blair HF, Makley JT, et al. Noninvasive grading of musculoskeletal tumors using PET. *J Nucl Med.* 1991;32:1508–1512.
12. Lodge MA, Lucas JD, Marsden PK, Cronin BF, O'Doherty MJ, Smith MA. A PET study of [18]FDG uptake in soft tissue masses. *Eur J Nucl Med.* 1999;26:22–30.
13. Boerner AR, Weckesser M, Herzog H, et al. Optimal scan time for fluorine-18 fluorodeoxyglucose positron emission tomography in breast cancer. *Eur J Nucl Med.* 1999;26:226–230.
14. Hustinx R, Smith RJ, Benard F, et al. Dual time point fluorine-18 fluorodeoxyglucose positron emission tomography: a potential method to differentiate malignancy from inflammation and normal tissue in the head and neck. *Eur J Nucl Med.* 1999;26:1345–1348.
15. Nakamoto Y, Higashi T, Sakahara H, et al. Delayed FDG PET scan for differentiation between malignant and benign lesions in the pancreas. *Cancer.* 2000;89:2547–2554.

16. Golshani-Hebroni SG, Bessmann SP. Hexokinase binding to mitochondria: a basis for proliferative energy metabolism. *J Bioenerg Biomembr.* 1997;29:331–338.

17. Board M, Humm S, Newsholme EA. Maximum activities of key enzymes of glycolysis, glutaminolysis, pentose phosphate pathway and tricarboxylic acid cycle in normal, neoplastic and suppressed cells. *Biochem J.* 1990;265:503–509.

18. Clavo AC, Brown RS, Wahl RL. Fluorodeoxyglucose uptake in human cancer cell lines is increased by hypoxia. *J Nucl Med.* 1995;36:1625–1632.

19. Higashi T, Tamaki N, Honda T, et al. Expression of glucose transporters in human pancreatic tumors compared with increased FDG accumulation in PET study. *J Nucl Med.* 1997;38:1337–1344.

20. Tamaki N, Yonekura Y, Yamashita K, et al. Relation of left ventricular perfusion and wall motion with metabolic activity in persistent defects on thallium-201 tomography in healed myocardial infarction. *Am J Cardiol.* 1988;62:202–208.

21. Younes M, Brown RW, Mody DR, Fernandez L, Laucirica R. GLUT1 expression in human breast carcinoma: correlation with known prognostic markers. *Anticancer Res.* 1995;15:2895–2898.

22. Tsai HJ, Wilson JE. Functional organization of mammalian hexokinases: both N- and C-terminal halves of the rat type II isozyme possess catalytic sites. *Arch Biochem Biophys.* 1996;329:17–23.

23. Wahl RL, Zasadny K, Helvie M, Hutchins GD, Weber B, Cody R. Metabolic monitoring of breast cancer chemohormonotherapy using positron emission tomography: initial evaluation. *J Clin Oncol.* 1993;11:2101–2111.

24. Torizuka T, Tamaki N, Inokuma T, et al. In vivo assessment of glucose metabolism in hepatocellular carcinoma with FDG PET. *J Nucl Med.* 1995;36:1811–1817.

25. Zasadny KR, Wahl RL. Standardized uptake values of normal tissues at PET with 2-[fluorine-18]-fluoro-2-deoxy-D-glucose: variations with body weight and a method for correction. *Radiology.* 1993;189:847–850.

26. Strauss LG. Fluorine-18 deoxyglucose and false-positive results: a major problem in the diagnostics of oncological patients. *Eur J Nucl Med.* 1996;23:1409–1415.

27. Shreve PD. Focal fluorine-18 fluorodeoxyglucose accumulation in inflammatory pancreatic disease. *Eur J Nucl Med.* 1998;25:259–264.

28. Zimny M, Buell U, Diederichs CG, Reske SN. False-positive FDG PET in patients with pancreatic masses: an issue of proper patient selection [letter]? *Eur J Nucl Med.* 1998;25:1352–1352.

29. Torizuka T, Zasadny KR, Recker B, Wahl RL. Untreated primary lung and breast cancers: correlation between F-18 FDG kinetic rate constants and findings of in vitro studies. *Radiology.* 1998;207:767–774.

30. Gupta N, Gill H, Graeber G, Bishop H, Hurst J, Stephens T. Dynamic positron emission tomography with F-18 fluorodeoxyglucose imaging in differentiation of benign from malignant lung/mediastinal lesions. *Chest.* 1998;114:1105–1111.

31. Smith TA. FDG uptake, tumour characteristics and response to therapy: a review. *Nucl Med Commun.* 1998;19:97–105.

32. Pauwels EK, Ribeiro MJ, Stoot JH, McCready VR, Bourguignon M, Maziere B. FDG accumulation and tumor biology. *Nucl Med Biol.* 1998;25:317–322.

33. Waki A, Kato H, Yano R, et al. The importance of glucose transport activity as the rate-limiting step of 2-deoxyglucose uptake in tumor cells in vitro. *Nucl Med Biol.* 1998;25:593–597.

34. Aloj L, Caraco C, Jagonda E, Eckelman WC, Neumann RD. Glut-1 and hexokinase expression: relationship with 2-fluoro-2-deoxy-D-glucose uptake in A431 and T47D cells in culture. *Cancer Res.* 1999;59:4709–4714.

35. Smith TA. Facilitative glucose transporter expression in human cancer tissue. *Br J Biomed Sci.* 1999;56:285–292.

36. Higashi T, Tamaki N, Torizuka T, et al. FDG uptake, GLUT-1 glucose transporter and cellularity in human pancreatic tumors. *J Nucl Med.* 1998;39:1727–1735.

37. Fukunaga T, Okazaki S, Koide Y, Isono K, Imazeki K. Evaluation of esophageal cancers using fluorine-18-fluorodeoxyglucose PET. *J Nucl Med.* 1998;39:1002–1007.

38. Paggi MG, Fanciulli M, Del Carlo C, Citro G, Carapella CM, Floridi A. The membrane-bound hexokinase as a potential marker for malignancy in human glioma. *J Neurosurg Sci.* 1990;34:209–213.